

SOLAR ABSORPTANCE AND THERMAL EMITTANCE OF PARTICLE HEAT CARRIERS IN A SOLAR DRIVEN BIOMASS PROCESS

Juan Pablo Rincon Duarte^{1,4}, Matteo Josse¹, Clarisse Lorreyte¹, Megan Kirschmeier¹,
Johannes Pernpeintner², Florian Sutter³, Martin Roeb¹, Christian Sattler^{1,4}

¹German Aerospace Center (DLR), Institute of Future Fuels, Cologne, Germany

²German Aerospace Center (DLR), Institute of Solar Research, Cologne, Germany

³German Aerospace Center (DLR), Institute of Solar Research, Almería, Spain

⁴RWTH University, Chair for Solar Fuel Production - Faculty of Mechanical Engineering, Aachen, Germany

ABSTRACT

Particle Heat Carriers (PHCs) are an innovative solution for the storage and transport of solar thermal energy. Integrating PHCs into a biomass pyrolysis process, whereby the PHCs are heated in a solar receiver, then sent to a pyrolysis reactor to supply the thermal energy for the process, is a unique approach for creating a solar-driven biomass pyrolysis process. To properly characterize the heat transfer in a directly irradiated solar receiver, it is essential to understand the PHC optical properties at different stages of the process. In this study, the reflectance of five different PHCs was measured at different process conditions: i) materials as received, ii) materials heated to 950 °C in air (simulating conditions in the solar receiver), and iii) materials mixed with wood chips and heated to 800 °C in nitrogen (simulating the pyrolysis stage). Reflectance measurements were performed in the spectral ranges of 0.25-2.5 and 2.5-16 μm to calculate the solar absorptance and the infrared thermal emittance, respectively.

Similar optical characteristics were observed for each process condition for particles initially dark in color (ex: bauxite, silicon carbide). However, when taking the as-received samples as a reference, significant increases in the solar absorptance were observed for 1) olivine, magnesium oxide and sand samples after being exposed to the pyrolysis conditions (increase by 23, 36 and 39 percentage points, respectively), and 2) the olivine sample after being heated in air at 950 °C (increase by 10 percentage points).

Keywords: Solar Thermal Energy, Particle Heat Carrier, Solar Absorptance, Thermal Emittance, Biomass Pyrolysis.

NOMENCLATURE

A_s	Near-normal hemispherical spectral absorptance of PHC sample
c	Speed of light in vacuum, 2.997×10^{-8} m/s
E_s	Thermal emittance of PHC sample
G_b	Solar direct irradiance on the Earth's surface
h	Planck constant, 6.63×10^{-34} Js
$I_{\#1}$	Detector intensity for the reference coupon #1
I_w	Detector intensity for the window
$I_{w,\#1}$	Detector intensity for the reference coupon #1 measured behind the window
$I_{w,s}$	Detector intensity for the specimen (the particle layer) measured behind the window
I_z	Detector intensity for the zeroline
k	Boltzmann constant, 1.38×10^{-23} J/K
M_{bb}	Blackbody spectral emittance
$R_{\#1}$	Certified near-normal hemispherical spectral reflectance of reference coupon #1 (SRS-05-020)
R_s	Near-normal hemispherical spectral reflectance
$R_{s,h}$	Solar-weighted hemispherical reflectance
T	PHC temperature

Greek Symbols

λ	Wavelength
ρ_w	Near-normal hemispherical reflectance of window
$\rho_{w,s}$	Near-normal hemispherical reflectance of PHC sample through the window
τ_w	Near-normal hemispherical transmittance of window

Acronyms

CSP	Concentrated Solar Power
DLR	German Aerospace Center
FTIR	Fourier-transform infrared spectrometer
MFC	Mass Flow Controller
MgO	Magnesium Oxide
PHC	Particle Heat Carrier
PYSOLO	Pyrolysis of biomass by concentrated Solar power
SiC	Silicon Carbide

1. INTRODUCTION

The European Union's chemical industry is facing a critical need to transition from reliance on fossil to renewable carbon sources, an essential shift to meet the ambitious targets of the Paris Climate Agreement (COP21). This industry-wide transformation requires not only the implementation of renewable energy sources, like solar power, but also the defossilisation of its processes, particularly in sourcing raw materials from renewable origins such as biomass. Pyrolysis of biomass has emerged as a promising process to obtain valuable products, such as biochar, syngas or biogas, while valorizing biowaste such as wood chips [1]. Nevertheless, this process is highly energy-intensive because it is endothermic and takes place at temperatures above 400 °C. In most conventional processes, the energy required comes from burning fossil fuels or biochar, which reduces the overall efficiency of the process. For this reason, research on solar-driven biomass pyrolysis is gaining interest [2–4], as CO₂ emissions from the combustion process currently used in state-of-the-art technology can be avoided. The Horizon Europe Project PYSOLO [5] looks at the integration of a solar-heated Particle Heat Carrier (PHC) in a biomass pyrolysis process. In this process, the PHC is used as a storage and transport medium for solar thermal energy [6]. The PHC is first heated in a solar receiver at temperatures near 800 °C, then sent to a pyrolysis reactor, where the thermal energy required for the pyrolysis reaction is released and, after separation from the solid products of this step (mostly biochar and ash), it is sent back to the solar receiver to close the loop. By contrast with conventional processes, PYSOLO's approach ensures a more complete utilization of biomass, thus enhancing both economic and environmental sustainability. For this application, abundant materials such as bauxite, magnesium oxide (MgO), olivine, sand, and silicon carbide (SiC) are possible PHC candidates. These materials, with the exception of MgO, have been analyzed by Kang et al. [7] in a circulation loop application for solar energy capture and storage. The study included a detailed analysis of thermochemical and mechanical properties, as well as an assessment considering health, safety, environmental and economic aspects. Olivine was found as the most favorable PHC for such application, but the optical properties were not considered in the study.

For a successful implementation of the PYSOLO technology, a PHC with optimal material properties must be selected. In addition to criteria such as specific heat capacity, mechanical stability, availability, environmental aspects, and

costs, the optical properties of the PHC are particularly relevant in the context of solar heat integration. The solar weighted absorptance and the thermal emittance of particles are crucial parameters to calculate the efficiency of a solar receiver [8].

Measurement of such properties for particle beds have been studied using different methods. Dispersive spectroscopy has been used to obtain directional-hemispherical reflectance and transmittance of sintered bauxite in the spectral range of i) 0.2-2.5 μm using disc-shaped samples [9], and ii) 0.38-15 μm using particles that were encased between two transparent windows [10]. The sintered bauxite samples in that study were characterized by a high solar absorptance (0.94-0.96), but this property can be modified due to sintering during the sample preparation process.

A different approach to determining the optical properties of spherical particles [11] included measurement techniques such as spectroscopic ellipsometry, scanning electron microscopy, atomic force microscopy and energy dispersive spectroscopy, which were applied to a thin film with the same material composition as the particles. This method was used for the analysis of alumina-mullite materials.

Previous studies [12, 13] have shown that the solar absorptance of sand is reduced when particles are exposed to fluidization at 900 °C in air, while this effect is not so relevant for SiC particles. Siegel et al. [8] performed an analysis with sintered bauxite particles, showing a decrease of the solar absorptance when particles are aged in air at 1000 °C. The absorptance drop of the sintered bauxite particles investigated by Sutter et al. [14] was as high as 14 percentage points when aged in air at 1000°C. Schroeder et al. [15] tested Carbohead HSP 40/70 sintered bauxite particles, which had an initial solar absorptance of 95%. In long-term experiments (representing a 30-year operating time), they measured a loss of 1 % after irradiation cycles and a loss of 4 % after thermal aging at 1000 °C.

The temperature-dependent emittance of sintered bauxite has also been studied at temperatures up to 457 °C using disc shaped samples [16] and packed beds of particles [17]. These measurements were made possible by special setups, including several mirrors to enable measurements with a Fourier-Transform Infrared Spectrometer (FTIR) at such temperatures. The total emittance of the sintered bauxite particles in [17] was between 0.89 and 0.96 and did not change monotonically with temperature, but different values were obtained when changing the chemical composition and particle size of the samples [16].

Infrared cameras in combination with thermocouples can also be used to estimate the emissivity of particles in high temperature granular flows, as shown by Bagepalli et al. [18].

As has been shown, measuring the optical properties of solid particles is a challenging task [19], but in recent years a guideline has been developed to obtain this information using spectrometers [19, 20]. The thermal emittance of solar particles can be calculated using reflectance measurements in the infrared range, which are usually performed at room temperature as described in [8, 19, 21, 22].

As the optical properties can vary during the different stages of the PYSOLO process, and due to the lack of data for materials such as olivine and MgO, the reflectance of the five chosen PHCs was measured at room temperature conditions in the spectral ranges of 0.25-2.5 μm and 2.5-16 μm . The reflectance results obtained were used to calculate the solar weighted absorptance of the PHCs and their infrared thermal emittance at 950 $^{\circ}\text{C}$. In this study, these two properties were analyzed for the different stages of the PYSOLO process, and a ranking was established to select the best PHCs for the process from the optical point of view.

2. MATERIALS AND METHODS

The five PHCs shown in Figure 1 were selected for this analysis: bauxite, silicon carbide (SiC), magnesium oxide (MgO), olivine and sand.



FIGURE 1: POSSIBLE PARTICLE HEAT CARRIERS FOR PYSOLO PROCESS (FROM LEFT TO RIGHT: BAUXITE, SiC, MgO, OLIVINE AND SAND).

To understand the expected optical characteristics of each PHC throughout the proposed PYSOLO solar pyrolysis process, it was important to simulate the state of the PHCs at each stage of the cyclic process. The process features two key components with two distinct operating environments: 1) the solar receiver, operating at approximately 950 $^{\circ}\text{C}$ in atmospheric conditions and 2) the pyrolysis reactor, operating at approximately 800 $^{\circ}\text{C}$ in an inert atmosphere with nitrogen gas. To accurately characterize the optical properties across the different process environments, four batches of each PHC were assessed:

1. particles as received directly from the supplier (as a reference)
2. particles heated in a furnace with air at 950 $^{\circ}\text{C}$ for 1 hour
3. particles pyrolyzed with the selected biomass (pine wood chips) with nitrogen at 800 $^{\circ}\text{C}$ for 1 hour
4. pyrolyzed particles (from the third batch) heated in a furnace with air at 950 $^{\circ}\text{C}$ for 1 hour

Note that case 4 was included to simulate the cyclic nature of the process and verify if the particles returned to the same state as in case 2 or if differences resulted from the pyrolysis process.

In addition to the measurement of the optical properties, which will be described in detail in the subsequent sections, microscopy was also implemented to provide a detailed analysis of the samples and help understand the observed variations in optical properties.

2.1 Material analysis

The choice of the different PHCs to be tested was carefully thought out to take into account the different constraints of the PYSOLO process [5]. The chemical composition and the particle size range of each PHC is summarized in TABLE 1.

TABLE 1: CHEMICAL COMPOSITION AND PARTICLE SIZE OF POSSIBLE PHC FOR PYSOLO PROCESS.

Composition/ Diameter	Bauxite	MgO	Olivine	SiC	Sand
SiO ₂	23.5	5	42		99.5
Al ₂ O ₃	76	1	0.4		0.13
Fe ₂ O ₃	3	4	7	0.2	
MgO		83	50		
CaO		5			
Cr ₂ O ₃			0.3		
NiO			0.3		
SiC				99	
C free				0.5	
Mean Particle Diameter / μm	250	250	250	300	250

Pine woodchip samples were used as the biomass source for the pyrolysis process. The woodchips were dried at 105 $^{\circ}\text{C}$ for 24 hours, and samples with an average size of 8 mm were obtained using a knife mill.

2.2 Preparation of samples

To compare how the optical properties of PHCs may vary during the different stages of the PYSOLO process, the four batches of samples described above were studied. Details of the experimental procedure for each sample are described in the following subsections.

2.2.1 Samples heated in air

The purpose of this analysis was to reproduce the solar receiver conditions. Therefore, 50 g of each PHC were placed in a Carbolite Gero RHF 14/35 furnace at 950 $^{\circ}\text{C}$ in an air atmosphere. A heating rate of 10 $^{\circ}\text{C}/\text{min}$ was employed, followed by a one-hour isothermal hold; the cooling step was not controlled. After reaching ambient temperature, the particles were removed from the furnace and stored in a closed container.

2.2.2 Samples exposed to pyrolysis conditions

To reproduce the pyrolysis conditions, a lab-scale setup was developed (see FIGURE 2) which included: i) a MKS mass flow controller (MFC) to set the nitrogen flow into the system, ii) a GERO tubular high temperature furnace (type Ro 50-250/13) to provide thermal energy for the process, iii) a 1.4841 steel tube to contain the particle sample as well as to control the atmospheric conditions in the system, iv) an isopropanol trap to clean the pyrolysis gas, and v) two K-type thermocouples to measure temperature in the central part of the furnace (next to the crucible containing the sample) and at the outlet of the steel tube, respectively.

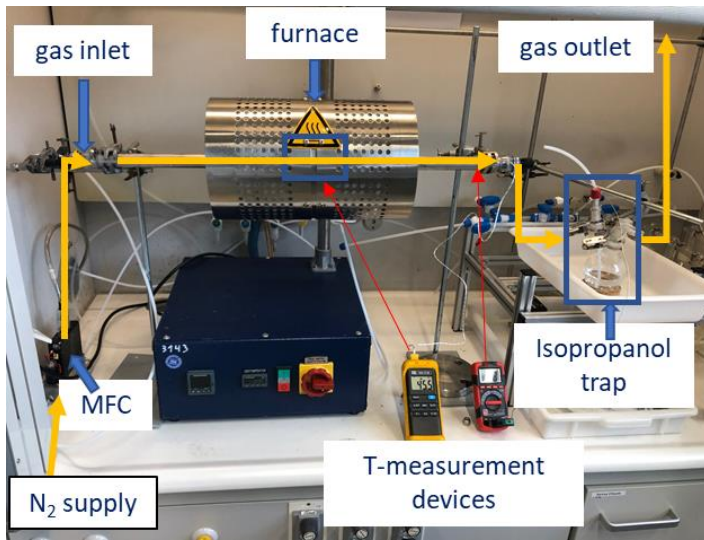


FIGURE 2: SETUP TO PREPARE SAMPLES EXPOSED TO PYROLYSIS CONDITIONS.

The PHC and biomass wood chips were placed together on a crucible plate with a mass range of 2.4-2.6 g and 0.4-0.6 g, respectively, as shown in FIGURE 3. This PHC-biomass ratio correlates to the ratio expected for the pyrolysis process. The biomass wood chips were positioned on top of the PHC sample to allow their separation after pyrolysis. The crucible was then inserted in the central part of the furnace, where the temperature distribution in the system was homogeneous, and the sample was heated to 800 °C using a heating rate of 10 °C/min. A constant mass flow of 200 ml/min of nitrogen was established throughout the test.



FIGURE 3: CRUCIBLE FILLED WITH SiC AND WOOD CHIPS.

After one hour, the furnace was switched off and, after cooling, the crucible was removed from the tube (FIGURE 4) and the biochar formed during the pyrolysis was carefully separated from the PHC. As the biochar pieces were noticeably larger than the PHC, it was possible to separate them using lab tweezers. The PHC was weighed after this process and the mass of the PHC differed by less than 2 % from the initial value. The PHC sample obtained was stored in a closed receptacle for further analysis.



FIGURE 4: CRUCIBLE AFTER PYROLYSIS WITH BIOCHAR AND SiC.

2.2.3 Heating of samples after pyrolysis

In the PYSOLO process, the PHCs complete the loop after pyrolysis by being heated again in the solar receiver. To verify whether the particle properties change during this step, further analyses were carried out. The post pyrolysis PHCs were collected and heated again in the furnace with the same conditions as the ones described in Section 2.2.1 .

2.3 Measurement procedure for optical properties of solid particles

The solar absorptance and the thermal emittance of the five PHCs were obtained following the SolarPaces guidelines developed by Sutter et al [19]. This method includes several reflectance and transmittance measurements, which are carried out in a spectrometer. For these measurements, standard white and gray references are needed, and the PHC samples must be placed inside a crucible which is closed with a glass window, as shown in FIGURE 5. The solar absorptance and the thermal emittance can be calculated from those measurement results. This procedure is explained in detail in the following subsections.



FIGURE 5: SAND PARTICLES INSIDE ASSEMBLY OF CRUCIBLE AND GLASS TO MEASURE THE OPTICAL PROPERTIES IN THE PERKIN-LAMBDA SPECTROMETER.

2.3.1 Solar absorptance

If the near-normal hemispherical spectral reflectance of a particle sample (R_s) is known and the particle sample is assumed opaque, its absorptance (A_s) can be calculated using Eq. (1).

$$A_s = 1 - R_s \quad (1)$$

To obtain R_s from Eq. (2), the near-normal hemispherical reflectance of the window (ρ_w) and of the particle layer measured through the window ($\rho_{w,s}$), as well as the near-normal hemispherical transmittance of the window (τ_w) are required.

$$R_s = \frac{\rho_{w,s} - \rho_w}{\tau_w^2 + \rho_w (\rho_{w,s} - \rho_w)} \quad (2)$$

ρ_w , $\rho_{w,s}$ (Eq. (3) and (4), respectively) and τ_w are calculated taking into account i) a certified near-normal hemispherical spectral of reference coupon SRS-05-020 ($R_{\#1}$), and ii) the results, which are obtained from the following set of measurements in a spectrometer:

1. zero line of the device (I_z)
2. window transmittance using the standard white reference (τ_w)
3. window reflectance with black cover (I_w)
4. base line with the standard grey reference ($I_{\#1}$)
5. window + standard grey reference ($I_{w,\#1}$)
6. PHC in crucible + window ($I_{w,s}$)

$$\rho_w = \frac{I_w - I_z \tau_w^2}{I_{\#1}} R_{\#1} \quad (3)$$

$$\rho_{w,s} = \frac{I_{w,s}}{I_{\#1}} R_{\#1} \quad (4)$$

These measurements were carried out at DLR in Cologne using a Perkin Elmer Lambda 950 spectrometer in the wavelength range between 250 and 2500 nm, which covers most of the solar spectrum. Note, however, that the results in the range from 250 to 319 nm are not considered for the calculation, since the window transmittance is rather low in this wavelength range.

The solar-weighted hemispherical reflectance ($R_{s,h}$) is obtained by weighting $R_s(\lambda)$ with the solar direct irradiance on the earth surface (G_b) according to Eq. (5), where G_b is given by the current standard ASTM G173-03 [23] for air mass 1.5.

$$R_{s,h} = \frac{\int_{320 \text{ nm}}^{2500 \text{ nm}} R_s(\lambda) \cdot G_b(\lambda) d\lambda}{\int_{320 \text{ nm}}^{2500 \text{ nm}} G_b(\lambda) d\lambda} \quad (5)$$

The solar-weighted hemispherical absorptance corresponds then to $1 - R_{s,h}$.

2.3.2 Thermal emittance

The thermal emittance of the PHC (E_s) was calculated in the infrared range using Eq. (6) [19, 21], where M_{bb} is the blackbody spectral emittance in $\text{W}/(\text{m}^2\mu\text{m})$ given by Eq. (7), in which the following universal physical constants are involved:

- c , the speed of light in vacuum ($2.997 \times 10^8 \text{ m/s}$)
- h , Planck's constant ($6.63 \times 10^{-34} \text{ Js}$)
- k , Boltzmann's constant ($1.38 \times 10^{-23} \text{ J/K}$)

$$E_s = \frac{\int_{2.5 \mu\text{m}}^{16 \mu\text{m}} [1 - R_s(\lambda)] M_{bb}(\lambda, T) d\lambda}{\int_{2.5 \mu\text{m}}^{16 \mu\text{m}} M_{bb}(\lambda, T) d\lambda} \quad (6)$$

$$M_{bb} = \frac{2\pi hc}{\lambda^5 [e^{\frac{hc}{\lambda kT}} - 1]} \quad (7)$$

R_s is calculated in a similar way as described in Section 2.3.1, but i) using a spectrometer in the infrared range and ii) including additional measurements with a diffuse gold standard [19]. These measurements were performed at DLR in Almería with a Frontier FTIR Perkin Elmer spectrometer for wavelengths between 2.5 and $16 \mu\text{m}$ and at room temperature conditions. Assuming that the optical behavior of the materials under investigation do not change with temperature, the thermal emittance at temperature of 950°C (corresponding to the receiver temperature) was computed with Eq. (6) and (7). It is important to emphasize that the results obtained using this method should be considered with caution, as the reflectance

spectrum of the material may be altered by high temperature conditions [24].

3 RESULTS AND DISCUSSION

3.1 Solar absorptance

FIGURE 6 shows the absorptance of the as-received materials as a function of wavelength. As expected, the darkest materials (i.e., bauxite and SiC) show the highest absorptance with values above 85 % for the entire measured spectrum. Olivine follows in third place with values higher than 60 %, while MgO and sand show absorptance values below 50 % in the wavelength range between 650 and $2500 \mu\text{m}$.

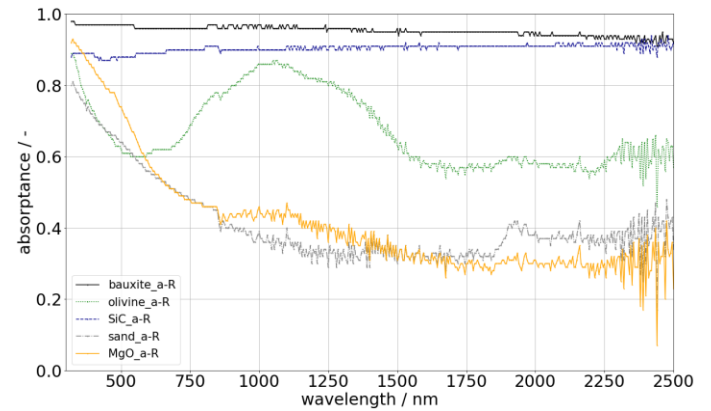


FIGURE 6: ABSORPTANCE OF MATERIALS AS RECEIVED AS FUNCTION OF THE WAVELENGTH.

When the samples were exposed to pyrolysis conditions, significant visual changes were observed for olivine, sand and MgO. As shown in FIGURE 7, these three materials became evidently darker due to their contact with the pyrolysis products, mainly with char. Interestingly, the olivine sample also changed its color when heated in air at 950°C , as it acquired a reddish-orange appearance (FIGURE 8), whereas the other four materials did not show considerable visual changes for the same experimental conditions.

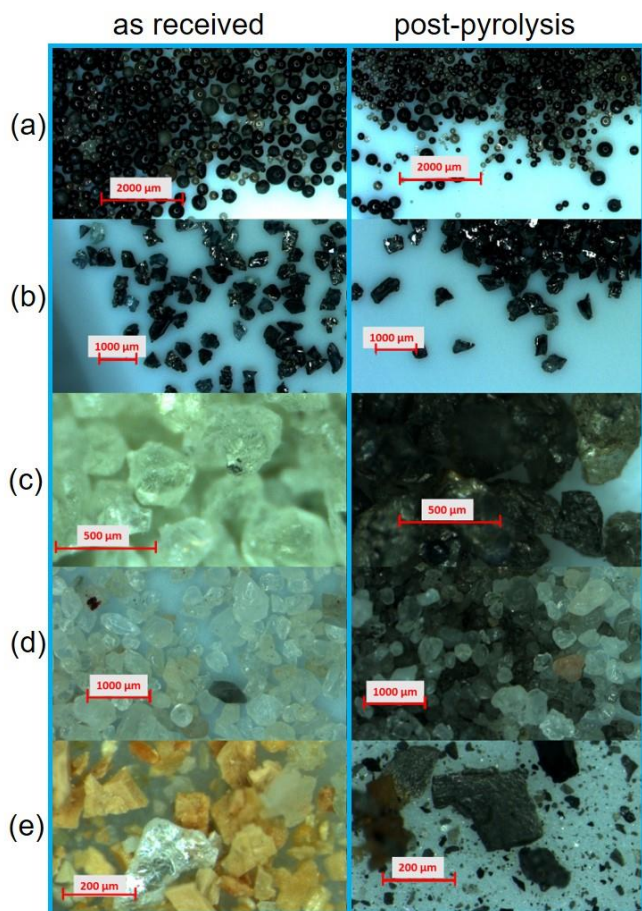


FIGURE 7: MICROSCOPY IMAGES OF SAMPLES OF BAUXITE (a), SiC (b), OLIVINE (c), SAND (d) AND MgO (e), SHOWING MATERIALS AS RECEIVED (LEFT) AND AFTER PYROLYSIS AT 800 °C (RIGHT). NOTE: THE SCALE USED FOR EACH PARTICLE HEAT CARRIER IS NOT THE SAME.

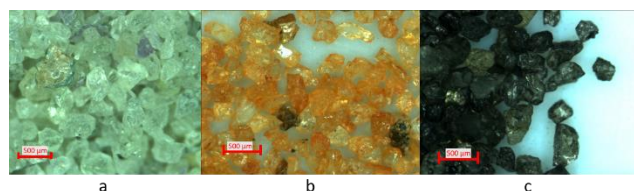


FIGURE 8: MICROSCOPY IMAGES OF OLIVINE SAMPLES: (a) AS RECEIVED, (b) AFTER HEATING IN AIR AT 950 °C, (c) AFTER PYROLYSIS AT 800 °C.

To simulate the final step of the PHCs in the PYSOLO process considering an open solar receiver, the pyrolyzed samples were heated again in air at 950 °C. As shown in FIGURE 9, the appearance of bauxite, MgO, olivine and sand changed significantly from the post-pyrolysis state. The black color gained during the pyrolysis was lost as char oxidized during the heating step. Considering the as-received materials as reference (FIGURE 1), bauxite passed from a dark-black- to a grayish-black color; MgO obtained its original orange-brown color; olivine changed its light green color to a reddish

appearance; sand became whiter; and no changes in SiC were observed.



FIGURE 9: PYROLYZED SAMPLES AFTER BEING HEATED IN AIR AT 950 °C (FROM LEFT TO RIGHT: BAUXITE, SiC, MgO, OLIVINE AND SAND).

TABLE 2 summarizes the solar-weighted absorptance of the four batches of samples. Taking as reference the as-received materials:

- the after-heated-in-air samples of SiC, bauxite and olivine increased their absorptance by 6, 1 and 10 percentage points, respectively, while a decrease by 3 percentage points was measured for sand, and no changes were observed for MgO;
- the pyrolyzed samples of olivine, MgO and sand increased their absorptance by 23, 36 and 39 percentage points, respectively, while for SiC and bauxite the absorptance values remained constant;
- the pyrolyzed samples subsequently exposed to heating under air conditions showed an increase in the absorptance for SiC, olivine and MgO (6, 11, and 1 percentage points, respectively), while for bauxite and sand a reduction of 3 and 6 percentage points were measured, respectively. The trends observed for sand and bauxite are consistent with the observations in [13] and [8], respectively. In the case of sand, the decrease in absorptance was associated with structural changes due to thermal aging, while in the case of bauxite, oxidation of metal ions in the constituents was associated with the color change and the reduction in absorptance. A similar decrease in the absorptance of bauxite samples was shown under comparable temperature conditions and longer thermal aging times [15].

These results are in good agreement with the above-presented visual observations.

TABLE 2: SOLAR-WEIGHTED ABSORPTANCE OF PHC SAMPLES CALCULATED IN THE 320-2500 nm RANGE.

PHC	As received	After heating in air at 950 °C	After pyrolysis at 800 °C	After pyrolysis and after heating in air at 950 °C
SiC	0.90	0.96	0.90	0.96
bauxite	0.96	0.97	0.96	0.93
olivine	0.70	0.80	0.93	0.81
MgO	0.53	0.53	0.89	0.54
sand	0.49	0.46	0.88	0.43

FIGURE 10 shows the absorptance of the four olivine samples. As observed, the absorptance results after reheating the pyrolyzed sample in air (red curve) are quite similar to those of the aged sample in air (orange curve).

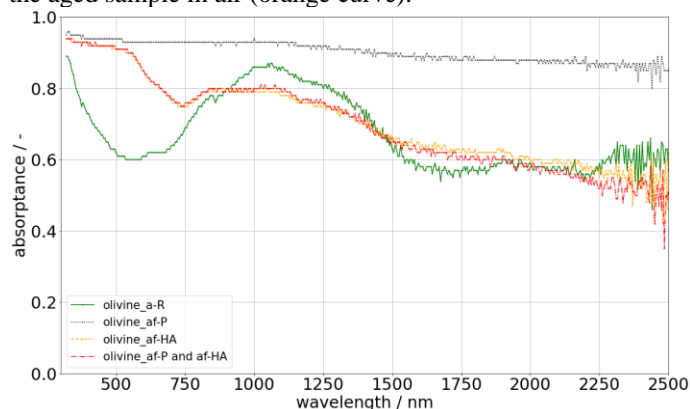


FIGURE 10: ABSORPTANCE OF OLIVINE SAMPLES AS FUNCTION OF THE WAVELENGTH.

For the solar receiver in the PYSOLO process, the as-received absorptance results are only important for fresh materials. After the second cycle, and depending on the configuration of the solar receiver:

- the absorptance results obtained after the pyrolysis step should be considered for a closed solar receiver operating in an inert atmosphere, since the char from the pyrolysis step will not be oxidized. For this scenario, the five PHCs are good candidates for the process. However, further experiments are needed to analyze whether the process of separating PHC and char, which is carried out after the pyrolysis stage, or the movement in the particle transport or inside the solar receiver can modify the surface characteristics of the post-pyrolysis particles. These points will be the subject of a later study;
- the absorptance results after aging in air the pyrolyzed samples must be considered for an open receiver. In this case, SiC, bauxite and olivine are the only viable PHC for the process, as absorptance of MgO and sand are less than 55 %. It is important to note that in an open receiver, the carbon i) attached to the particles or ii) that failed to separate in the separator, will combust, modifying the CO₂ content in the receiver atmosphere, which in turn may affect the absorptance of the particles differently. The CO₂ content depends mainly on the separation efficiency of the particle-char separator. In the case of low separation efficiency and observed disadvantages due to oxidation in an atmosphere with high CO₂ content, it is foreseen to implement a combustion unit upstream of the solar receiver [25]. This study is currently being developed in detail within the framework of PYSOLO.

3.2 Thermal emittance

The thermal emittance of the five PHCs (as received, after heated in air at 950 °C, and after pyrolysis at 800 °C) was calculated in the wavelength range between 2.5 and 16 μm. These results are summarized in TABLE 3. Since we did not observe significant changes between absorptance after heating of as-received and pyrolyzed PHC, we do not expect significant changes for thermal emittance. For this reason, we did not perform reflectance measurements for the pyrolyzed samples after heating in air at 950°C.

Considering as reference the as-received samples:

- the samples aged in air at 950 °C of bauxite, olivine, sand and MgO showed a decrease in their thermal emittance of 3, 10, 5 and 11 percentage points, respectively, while SiC showed an increase of 2 percentage points.
- the thermal emittance of the after-pyrolysis samples of olivine, sand and MgO increased by 4, 7 and 29 percentage points, respectively, while a decrease of 2 percentage points was observed for bauxite. The value of SiC did not change.

TABLE 3: THERMAL EMITTANCE OF PHC SAMPLES CALCULATED IN THE 2.5-16 μm RANGE.

PHC	As received	After heating in air at 950°C	After pyrolysis at 800°C
SiC	0.90	0.92	0.90
bauxite	0.91	0.88	0.89
olivine	0.85	0.74	0.89
MgO	0.63	0.53	0.92
sand	0.77	0.72	0.84

For CSP systems seeking immediate heat utilization, high absorptance combined with high emittance allows for optimal solar energy capture and effective thermal radiation release post-sunlight absorption [22]. In the PYSOLO process, this scenario can occur when PHC is sent from the solar receiver to the pyrolyzer in a short period of time. In this case, SiC and bauxite are the best candidates if an open solar receiver is considered, while MgO, SiC, bauxite and olivine could be used when a closed solar receiver is contemplated.

However, if higher heat retention between the solar receiver and the pyrolyzer is envisaged, PHCs with low thermal emittance are more appropriate for such an application. In this case, olivine and sand are very interesting options for the PYSOLO process if an open and closed receiver are considered, respectively.

The results of thermal emittance obtained in this study should be considered with caution, and future research should include special measuring equipment in high temperature conditions as in [11, 17, 24].

4 CONCLUSION

In this study, the solar absorptance and thermal emittance of bauxite, SiC, olivine, sand and MgO were determined. The

feasibility of integrating these PHCs into the PYSOLO process was analyzed.

The absorptance and emittance of olivine, sand and MgO are significantly affected by the process conditions. For example, samples exposed to pyrolysis conditions increased their absorbance and emittance values above 88 % and 84 %, respectively. Olivine, MgO and sand samples aged in air at 950 °C showed a decrease in thermal emittance of 9, 10 and 5 percentage points, respectively.

The gain in absorptance and emittance due to the char of the pyrolysis stage is lost if PHCs are oxidized in air, which is the case for an open solar receiver. Therefore, the selection of the best PHC candidate will also depend on the type of solar receiver considered for the process (as well as other material properties).

For all conditions tested, SiC and bauxite showed high absorptance and emittance (above 90 % and 88 %, respectively), and are good PHCs in a scenario where the heat gained in the solar receiver is released in the pyrolyzer in a short period of time. In the case of higher heat retention between the solar receiver and the pyrolyzer, olivine and sand become interesting PHCs for the PYSOLO process considering an open and closed solar receiver, respectively.

ACKNOWLEDGEMENTS

This study is funded by the European Union. Views and opinions expressed are however those of the author(s) only and do not necessarily reflect those of the European Union or the European Climate, Infrastructure and Environment Executive Agency (CINEA). Neither the European Union nor the granting authority can be held responsible for them. The PYSOLO project receives funding from the Horizon Europe Framework Programme under grant agreement number 101118270.

The authors are very thankful to Giacomo Lombardi and Andrea Maria Rizzo for facilitating the PHC and biomass samples; to Lamark de Oliveira and David Vellas for their support with the preparation of the samples in Cologne; and to Eckard Lüpfer and Marco Binotti for the valuable discussions during this study.

REFERENCES

- [1] T. S. Tanoh, A. Ait Oumeziane, J. Lemonon, F. J. Escudero Sanz, and S. Salvador, "Green Waste/Wood Pellet Pyrolysis in a Pilot-Scale Rotary Kiln: Effect of Temperature on Product Distribution and Characteristics," *Energy Fuels*, vol. 34, no. 3, pp. 3336–3345, 2020, doi: 10.1021/acs.energyfuels.9b04365.
- [2] M. Raza *et al.*, "Progress of the Pyrolyzer Reactors and Advanced Technologies for Biomass Pyrolysis Processing," *Sustainability*, vol. 13, no. 19, p. 11061, 2021, doi: 10.3390/su131911061.
- [3] H. Grassmann *et al.*, "Solar Biomass Pyrolysis with the Linear Mirror II," *SGRE*, vol. 06, no. 07, pp. 179–186, 2015, doi: 10.4236/sgre.2015.67016.
- [4] S. Morales, R. Miranda, D. Bustos, T. Cazares, and H. Tran, "Solar biomass pyrolysis for the production of bio-fuels and chemical commodities," *Journal of Analytical and Applied Pyrolysis*, vol. 109, pp. 65–78, 2014, doi: 10.1016/j.jaap.2014.07.012.
- [5] <https://pysolo.eu/>, *Horizon Europe Project PYSOLO*.
- [6] M. A. Amjed, F. Sobic, M. C. Romano, T. Faravelli, and M. Binotti, "Techno-economic analysis of a solar-driven biomass pyrolysis plant for bio-oil and biochar production," *Sustainable Energy Fuels*, vol. 8, no. 18, pp. 4243–4262, 2024, doi: 10.1039/d4se00450g.
- [7] Q. Kang, G. Flamant, R. Dewil, J. Baeyens, H. L. Zhang, and Y. M. Deng, "Particles in a circulation loop for solar energy capture and storage," *Particuology*, vol. 43, pp. 149–156, 2019, doi: 10.1016/j.partic.2018.01.009.
- [8] N. Siegel, M. Gross, C. Ho, T. Phan, and J. Yuan, "Physical properties of solid particle thermal energy storage media for concentrating solar power applications," *Energy Procedia*, vol. 49, no. 1, pp. 1015–1023, 2014.
- [9] Jingjing Chen, Asim Riaz, Mahdiar Taheri, Apurv Kumar, Joe Coventry, and Wojciech Lipiński, "Optical and radiative characterisation of alumina–silica based ceramic materials for high-temperature solar thermal applications," *Journal of Quantitative Spectroscopy and Radiative Transfer*, vol. 272, p. 107754, 2021, doi: 10.1016/j.jqsrt.2021.107754.
- [10] C. Chen, C. Yang, D. Ranjan, P. G. Loutzenhiser, and Z. M. Zhang, "Spectral Radiative Properties of Ceramic Particles for Concentrated Solar Thermal Energy Storage Applications," *International Journal of Thermophysics*, vol. 41, no. 11, p. 152, 2020, doi: 10.1007/s10765-020-02733-5.
- [11] Jingjing Chen, Vincent M. Wheeler, Boqing Liu, Apurv Kumar, Joe Coventry, and Wojciech Lipiński, "Optical characterisation of alumina–mullite materials for solar particle receiver applications," *Solar Energy Materials and Solar Cells*, vol. 230, p. 111170, 2021, doi: 10.1016/j.solmat.2021.111170.
- [12] M. Díaz-Heras, A. Calderón, M. Navarro, J. A. Almendros-Ibáñez, A. I. Fernández, and C. Barreneche, "Characterization and testing of solid particles to be used in CSP plants: Aging and fluidization tests," *Solar Energy Materials and Solar Cells*, vol. 219, p. 110793, 2021, doi: 10.1016/j.solmat.2020.110793.
- [13] A. Palacios, A. Calderón, C. Barreneche, J. Bertomeu, M. Segarra, and A. I. Fernández, "Study on solar absorptance and thermal stability of solid particles materials used as TES at high temperature on different aging stages for CSP applications," *Solar Energy Materials and Solar Cells*, vol. 201, p. 110088, 2019, doi: 10.1016/j.solmat.2019.110088.
- [14] F. Sutter *et al.*, "Thermal and environmental durability of novel particles for Concentrated solar thermal technologies," *Solar Energy Materials and Solar Cells*, vol. 281, p. 113316, 2025, doi: 10.1016/j.solmat.2024.113316.
- [15] N. Schroeder, H. E. Bush, and K. Albrecht, "Assessment of Particle Candidates for Falling Particle Receiver Applications Through Irradiance and Thermal Cycling," *J*

- Sol Energy-T Asme*, vol. 147, no. 3, p. 31012, 2025, doi: 10.1115/1.4067497.
- [16] Jingjing Chen, Juan F. Torres, Sahar Hosseini, Apurv Kumar, Joe Coventry, and Wojciech Lipiński, "High-temperature optical and radiative properties of alumina-silica-based ceramic materials for solar thermal applications," *Solar Energy Materials and Solar Cells*, vol. 242, p. 111710, 2022, doi: 10.1016/j.solmat.2022.111710.
 - [17] C. Chen, C. Yang, K. Pan, D. Ranjan, P. G. Loutzenhiser, and Z. M. Zhang, "Temperature-dependent spectral emittance of bauxite and silica particle beds," *Experimental Heat Transfer*, vol. 36, no. 6, pp. 826–844, 2023, doi: 10.1080/08916152.2022.2080301.
 - [18] Malavika V. Bagepalli, Shin Young Jeong, Joshua D. Brooks, Zhuomin M. Zhang, Devesh Ranjan, and Peter G. Loutzenhiser, "Experimental characterization of extreme temperature granular flows for solar thermal energy transport and storage," *Solar Energy Materials and Solar Cells*, vol. 248, p. 112020, 2022, doi: 10.1016/j.solmat.2022.112020.
 - [19] SolarPaces, Ed., *Method to evaluate the reflectance, absorptance and emittance of particles for concentrating solar power technology*: SolarPACES, 2022.
 - [20] F. Sutter *et al.*, "Round Robin Test of Absorptance and Emittance of Particles for CSP," *SolarPACES Conf Proc*, vol. 1, 2023, doi: 10.52825/solarpaces.v1i.629.
 - [21] S. Caron *et al.*, "Laboratory intercomparison of solar absorptance and thermal emittance measurements at room temperature," *Solar Energy Materials and Solar Cells*, vol. 238, p. 111579, 2022, doi: 10.1016/j.solmat.2022.111579.
 - [22] K. Bum Han *et al.*, "Optical properties enhancement of thermal energy media for consistently high solar absorptivity," *Sol Energy*, vol. 274, p. 112603, 2024, doi: 10.1016/j.solener.2024.112603.
 - [23] *ASTM G173-03 Standard Tables for Reference Solar Spectral Irradiances: Direct Normal and Hemispherical on 37° Tilted Surface*, ASTM International, 2003.
 - [24] P. Giraud, J. Braillon, C. Delord, and O. Raccurt, "Development of optical tools for the characterization of selective solar absorber at elevated temperature," *AIP Conference Proceedings*, vol. 1734, no. 1, p. 130008, 2016, doi: 10.1063/1.4949218.
 - [25] M. Binotti *et al.*, "Solar-driven Biomass Pyrolysis Plant for Negative-Emission Biofuels Production," 2024.